Title here

Elio Campitelli * and Leandro Díaz

CIMA UBA blablabla

Carolina Vera

Corresponding author: Elio Campitelli,elio.campitelli@cima.fcen.uba.ar

ABSTRACT

Enter the text of your abstract here. This is a sample American Meteorological Society (AMS) LaTeX template. This document provides authors with instructions on the use of the AMS LaTeX template. Authors should refer to the file amspaper.tex to review the actual LaTeX code used to create this document. The template.tex file should be modified by authors for their own manuscript.

Significance statement. This is significant becasue I wrote it.

1. Introduction

yada yada SAM yada yada circulation.. yada yada so important. yada yada many impacts.

2. Methods

1) DATA

We used monthly geopotential height at 2.5 longitude by 2.5 latitude resolution from ERA5 (Hersbach et al.) for the period 1979 to 2018 (inclusive).

Monthly temperature NOAA Global Surface Temperature (NOAAGlobalTemp) 5.0 degree latitude x 5.0 degree longitude global grid (Vose et al. 2012; Smith et al. 2008). The same analysis was carried out using CRUTEM4 (Osborn and Jones 2014) (not shown).

We used monthly precipitation data from CPC Merged Analysis of Precipitation (Xie and Arkin 1997) 2.5 degree latitude x 2.5 degree longitude.

2) DEFINITION OF INDEXES

We defined the Southern Annular Mode (SAM) as the leading EOF of the monthly anomalies of geopotential field at 700 hPa south of 20°S (citation?). The EOF was performed by computing the Singular Value Decomposition of the data matrix consisting in 481 rows and 4176 columns (144 points of longitude and 29 points of latitude). The values where weighted by the square root of the cosine of latitude to account for the non-equal area of each gridpoint (Chung and Nigam 1999). This same method was used at the rest of the levels considered in this paper.

To separate between the zonally symmetric and asymmetric components of the SAM, we computed the zonal mean and anomalies of the full SAM spatial pattern. The results are shown in

Figure 5 for 700hPa. The full spatial signal ($\mathrm{EOF}_1(\lambda,\phi)$) is the sum of the zonally asymmetric ($\mathrm{EOF}_1^*(\lambda,\phi)$) and symmetric ($[\mathrm{EOF}_1](\lambda,\phi)$) components. We then compute the "Full", "Asymmetric" and "Symmetric" indexes, by regressing each geopotential field on these patterns (weighting by the cosine of latitude).

The three indexes are normalised by dividing them by the standard deviation of the "Full" index at each level. This means that comparing the magnitude between indexes is meaningful, but it also means that not every index will have unit standard deviation.

3) Significance

We adjusted p-values for False Detection Rate following Wilks (2016).

3. Results

Sem tortor mus non tristique augue. Donec vel feugiat sit aliquet lorem dui lobortis dolor risus. Proin, ac eu, mauris. Dolor id habitasse, curabitur platea ante. Rhoncus volutpat himenaeos vestibulum ut bibendum felis non. Ligula placerat ac luctus ad. Ante, lorem volutpat eu dapibus pharetra arcu. Sollicitudin eu tortor amet. Maecenas nulla euismod ac suspendisse metus. A ac, hendrerit, sit sollicitudin ac primis ullamcorper tempor id, mauris. Sem diam, sem curabitur. Risus, nullam vel diam hendrerit massa nec non. Donec amet amet ultrices ac taciti aliquam. Enim arcu et sed sit.

Ligula sed sociosqu imperdiet magna curabitur, et, elit lobortis ut, sed. Placerat id eros quis vivamus sed, in felis. Egestas phasellus at sagittis sed senectus malesuada. Vestibulum at pretium elementum id, facilisi. Porttitor luctus vel tempus diam nec per, nibh nisi. Viverra turpis nisl sed nec varius, et ridiculus in amet. Amet sapien nec convallis arcu dis et mauris dolor. Vestibulum, in, in tincidunt tellus risus class quisque, augue feugiat.

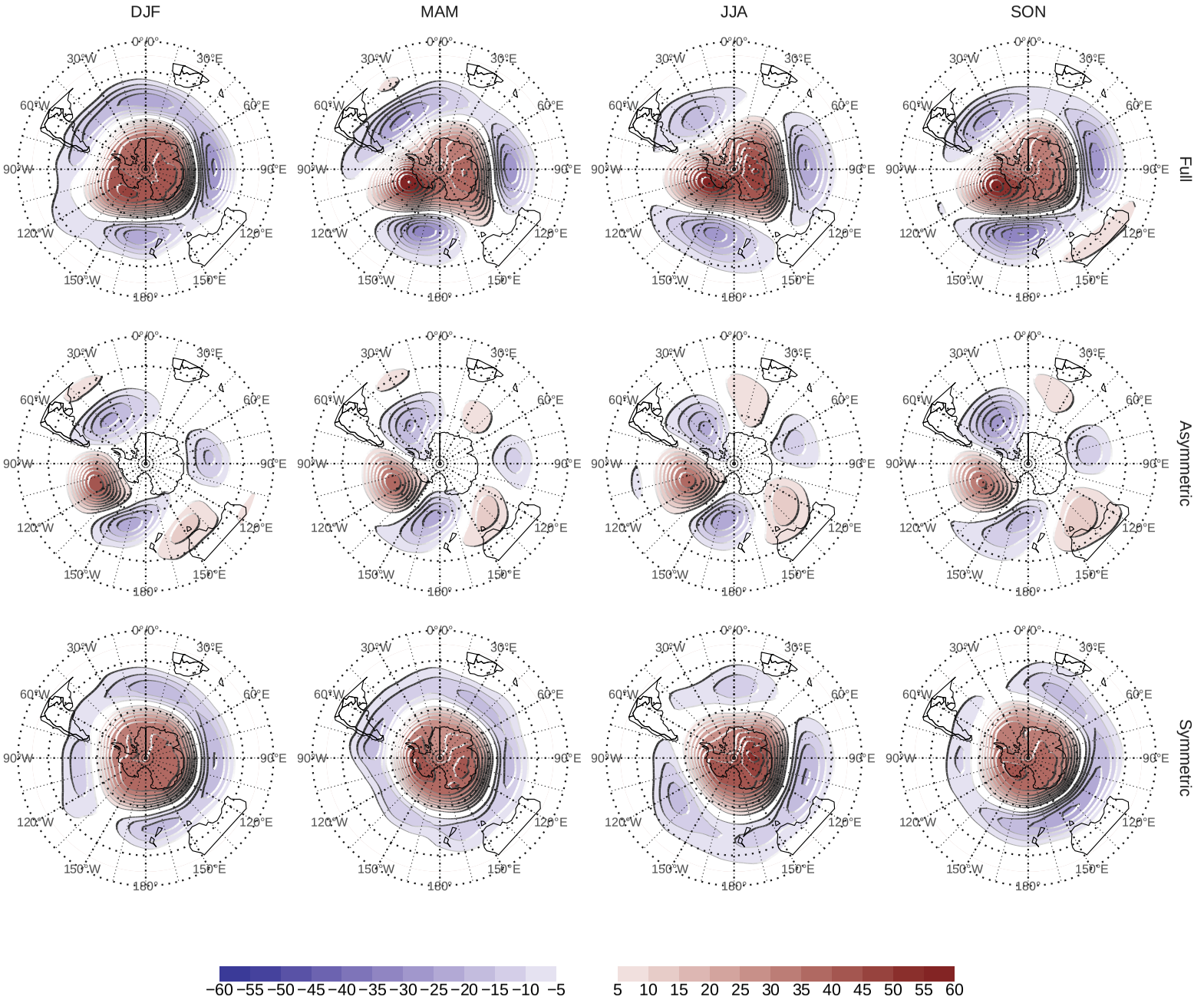

FIG. 1. Seasonal regression patterns of geopotential height at 700 hPa with the Full, Asymmetric and Symmetric SAM. The regression patterns for Asymmetric and Symmetric SAM are the result of one multiple regression using both indices, not of two simple regressions involving each index by itself.

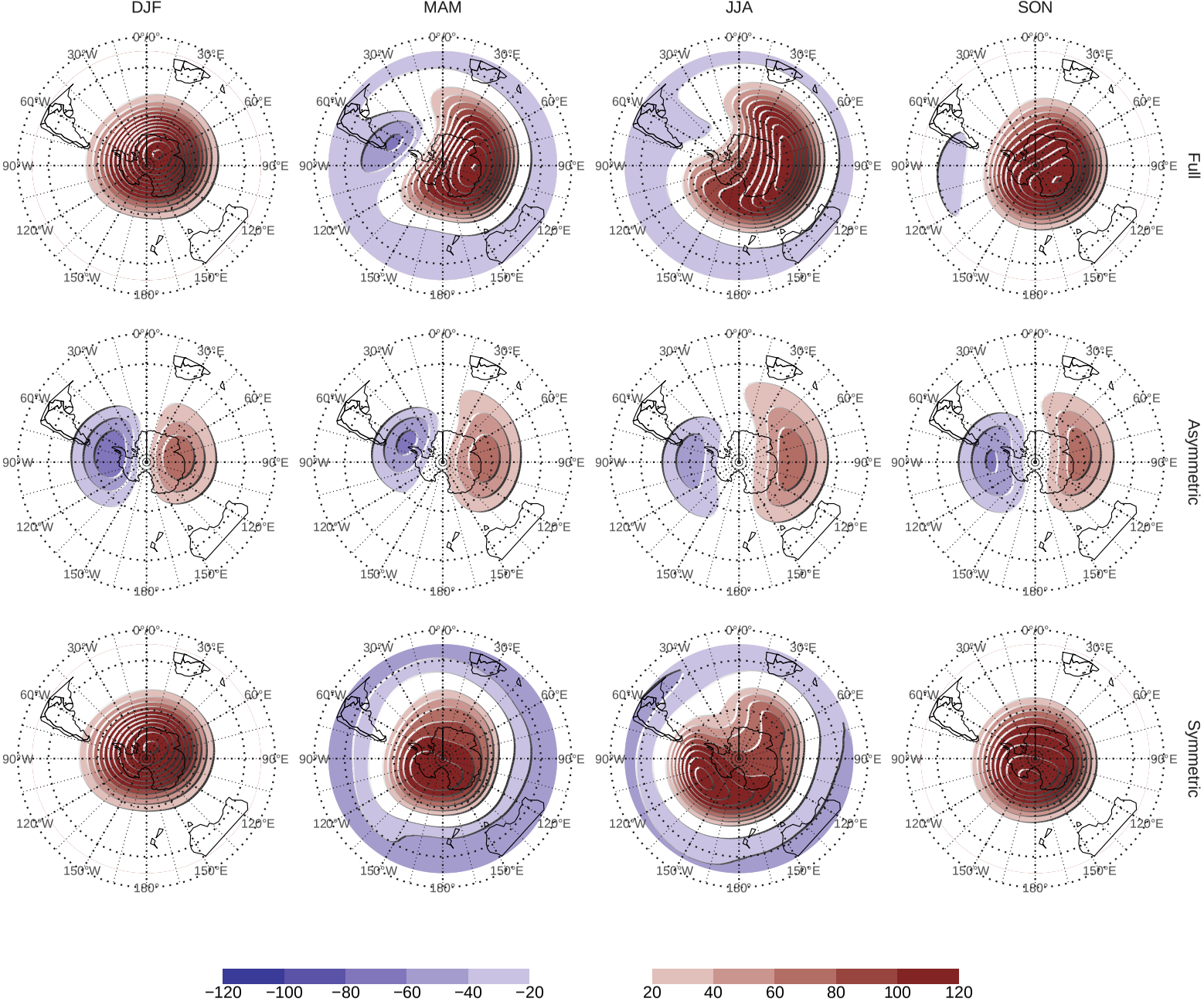

FIG. 2. Seasonal regression patterns of geopotential height at 30 hPa with the Full, Asymmetric and Symmetric SAM. The regression patterns for Asymmetric and Symmetric SAM are the result of one multiple regression using both indices, not of two simple regressions involving each index by itsef.

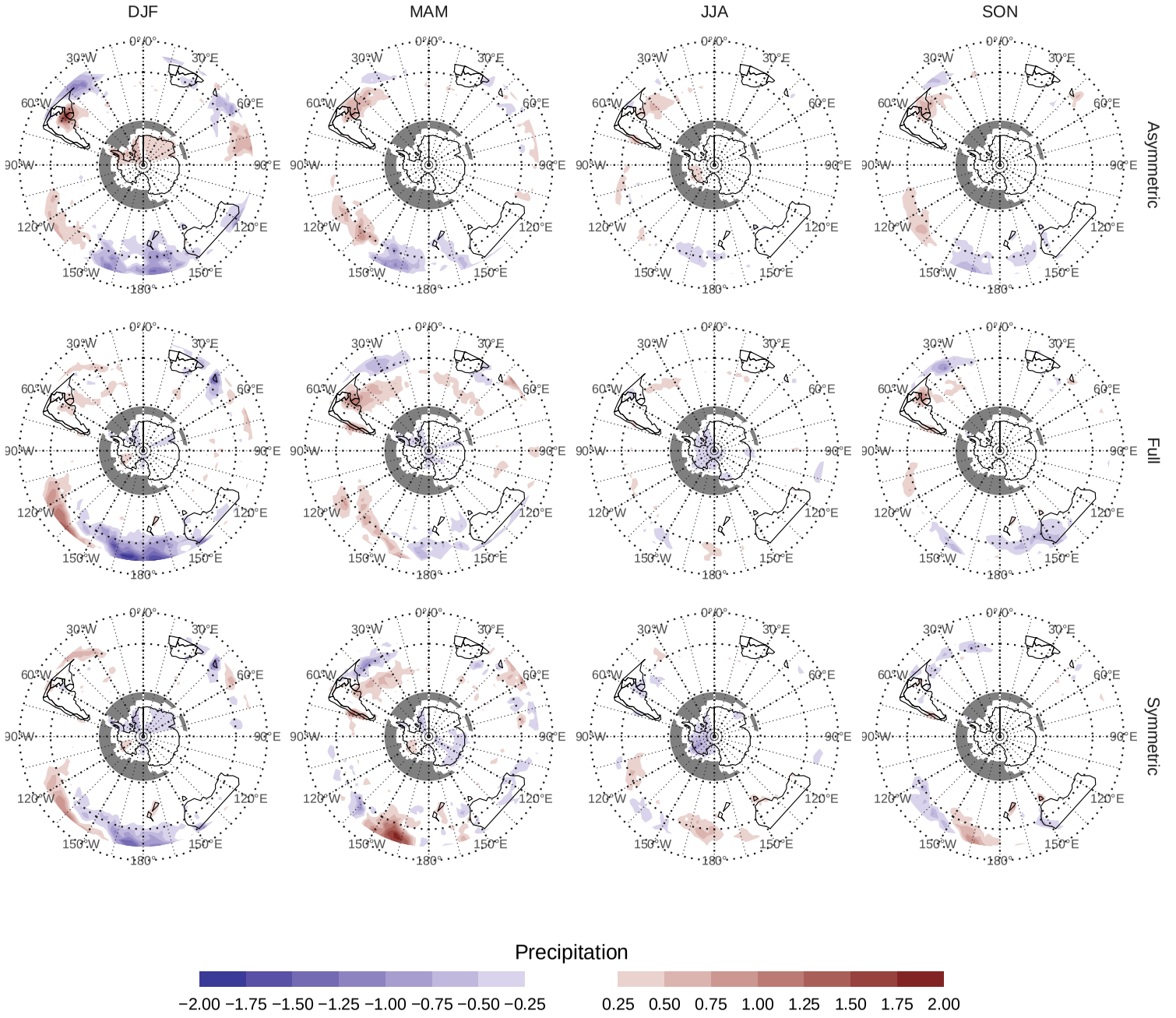

FIG. 3. Regression pattern of precipiation with Asymmetric and Symmetric SAM. P-values smaller than 0.05 (controlling for Flase Detection Rate) as hatched areas.

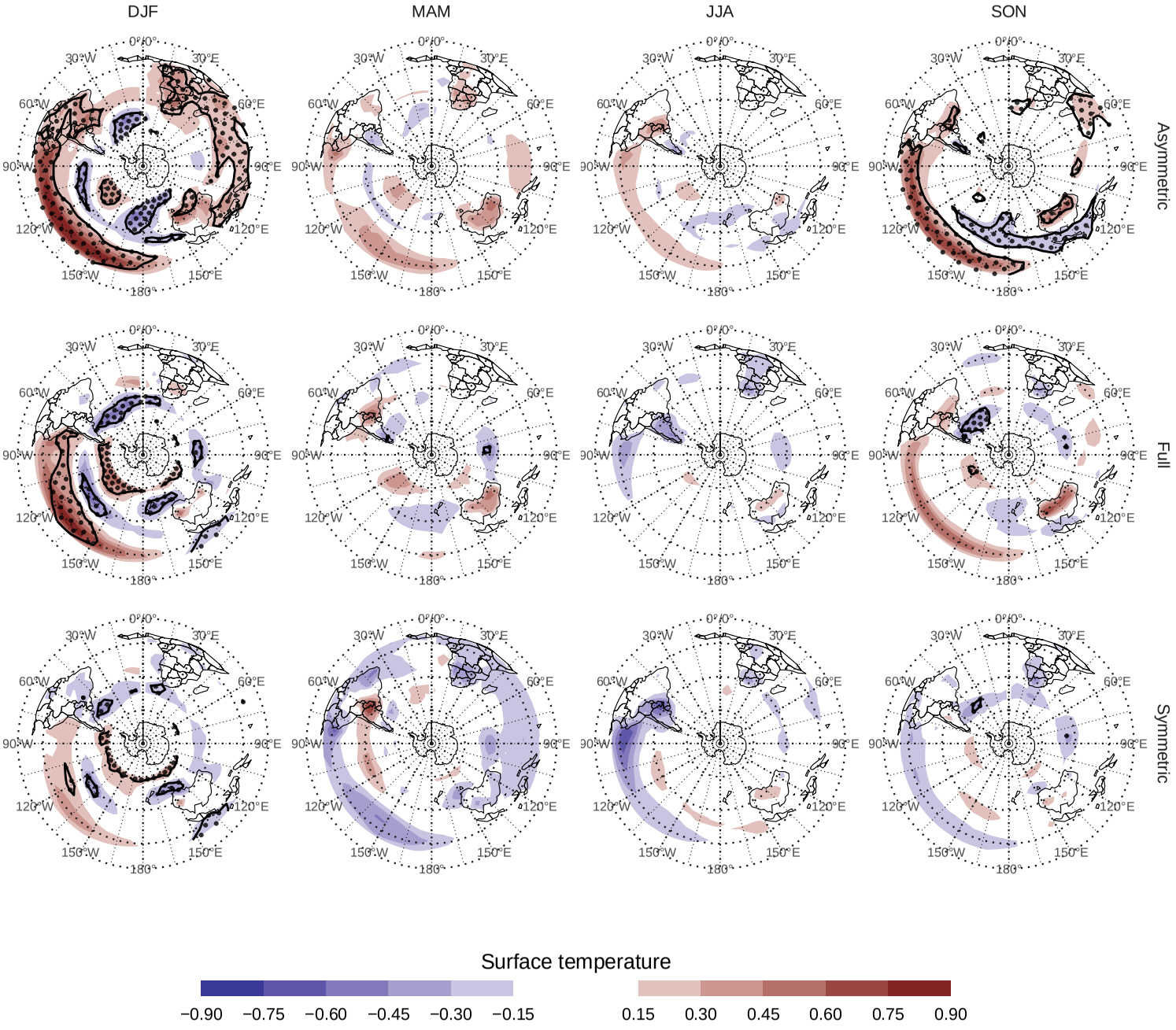

FIG. 4. Regression pattern of surface temperature with Asymmetric and Symmetric SAM. P-values smaller than 0.05 (controlling for Flase Detection Rate) as hatched areas.

Acknowledgments. CMAP Precipitation data provided by the NOAA/OAR/ESRL PSL, Boulder, Colorado, USA, from their Web site at https://psl.noaa.gov/

NOAA Global Surface Temperature (NOAAGlobalTemp) data provided by the NOAA/OAR/ESRL PSL, Boulder, Colorado, USA, from their Web site at https://psl.noaa.gov/

References

Chung, C., and S. Nigam, 1999: Weighting of geophysical data in Principal Component Analysis. *Journal of Geophysical Research: Atmospheres*, **104 (D14)**, 16 925–16 928, doi: 10.1029/1999JD900234.

Hersbach, H., and Coauthors, ????: The ERA5 global reanalysis. *Quarterly Journal of the Royal Meteorological Society*, **n/a (n/a)**, doi:10.1002/qj.3803.

Osborn, T. J., and P. D. Jones, 2014: The CRUTEM4 land-surface air temperature data set: Construction, previous versions and dissemination via Google Earth. *Earth System Science Data*, **6 (1)**, 61–68, doi:10.5194/essd-6-61-2014.

Smith, T. M., R. W. Reynolds, T. C. Peterson, and J. Lawrimore, 2008: Improvements to NOAA's Historical Merged Land–Ocean Surface Temperature Analysis (1880–2006). *J. Climate*, **21 (10)**, 2283–2296, doi:10.1175/2007JCLI2100.1.

Vose, R. S., and Coauthors, 2012: NOAA's Merged Land–Ocean Surface Temperature Analysis. *Bull. Amer. Meteor. Soc.*, **93 (11)**, 1677–1685, doi:10.1175/BAMS-D-11-00241.1.

Wilks, D. S., 2016: "The Stippling Shows Statistically Significant Grid Points": How Research Results are Routinely Overstated and Overinterpreted, and What to Do about It. *Bull. Amer. Meteor. Soc.*, **97 (12)**, 2263–2273, doi:10.1175/BAMS-D-15-00267.1.

Xie, P., and P. A. Arkin, 1997: Global Precipitation: A 17-Year Monthly Analysis Based on Gauge Observations, Satellite Estimates, and Numerical Model Outputs. *Bull. Amer. Meteor. Soc.*, **78 (11)**, 2539–2558, doi:10.1175/1520-0477(1997)078<2539:GPAYMA>2.0.CO;2.

APPENDIX

Extra figures

LIST OF FIGURES

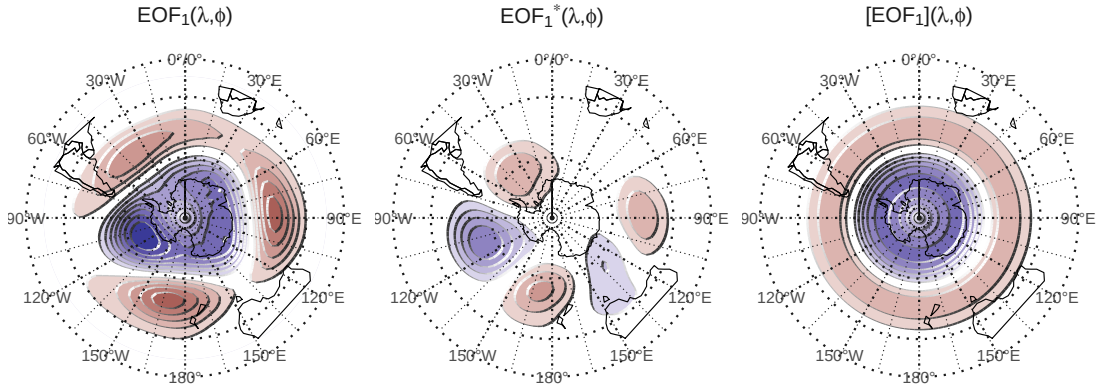

FIG. 5. Spatial patterns of the first EOF of 700 hPa geopotential height. Full field (left), zonally asymmetric component (middle) and zonally symmetric component (right). Arbitrary units.

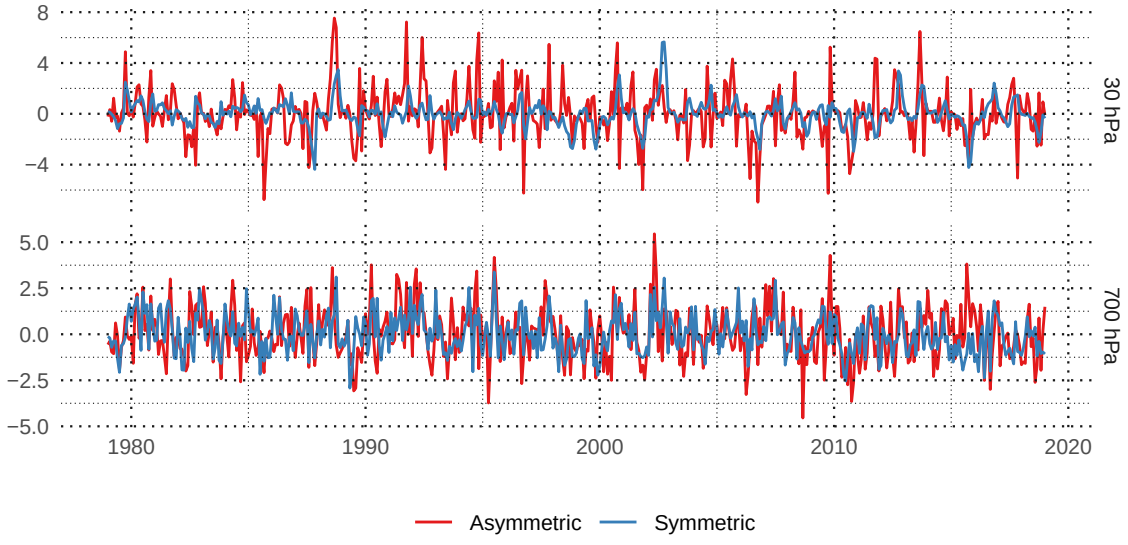

FIG. 6. Time series for the asymmetric SAM and symmetric SAM.

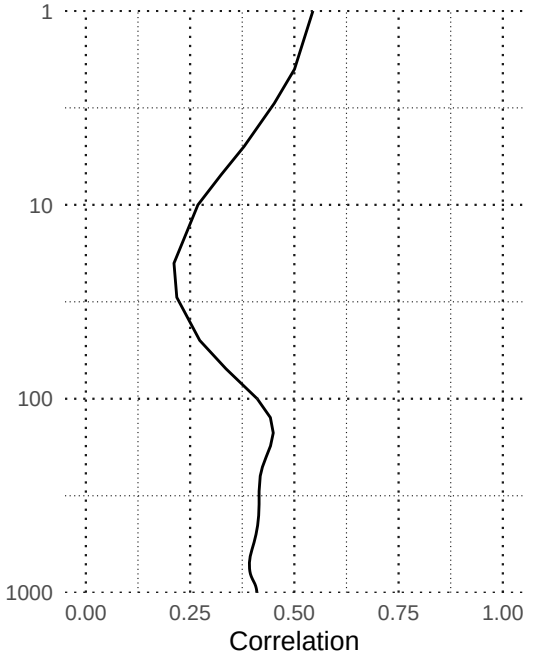

FIG. 7. Correlation between the Symmetric and Asymmetric SAM at each level.

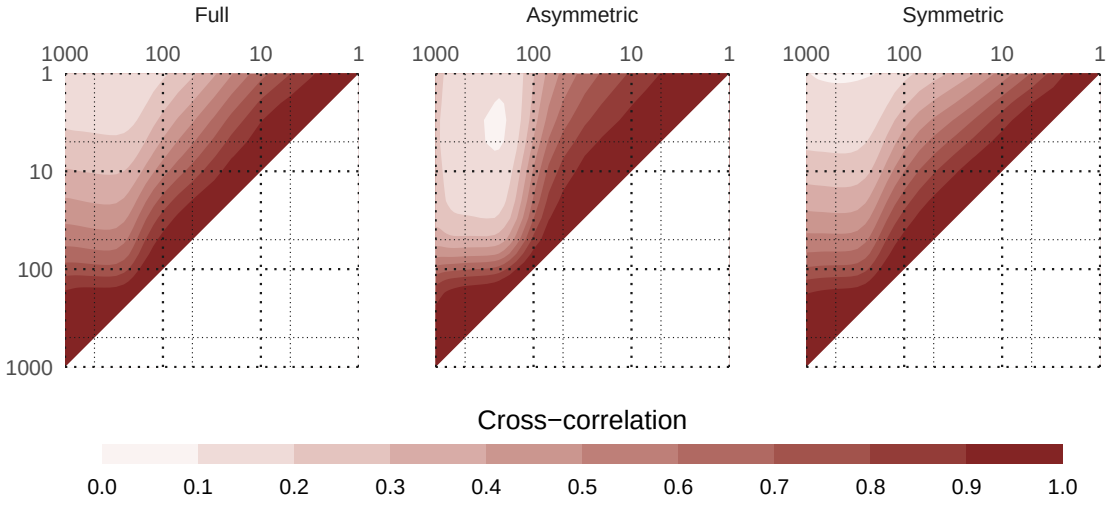

FIG. 8. Cross correlation between levels of the Full, Asymmetric and Symmetric SAM.

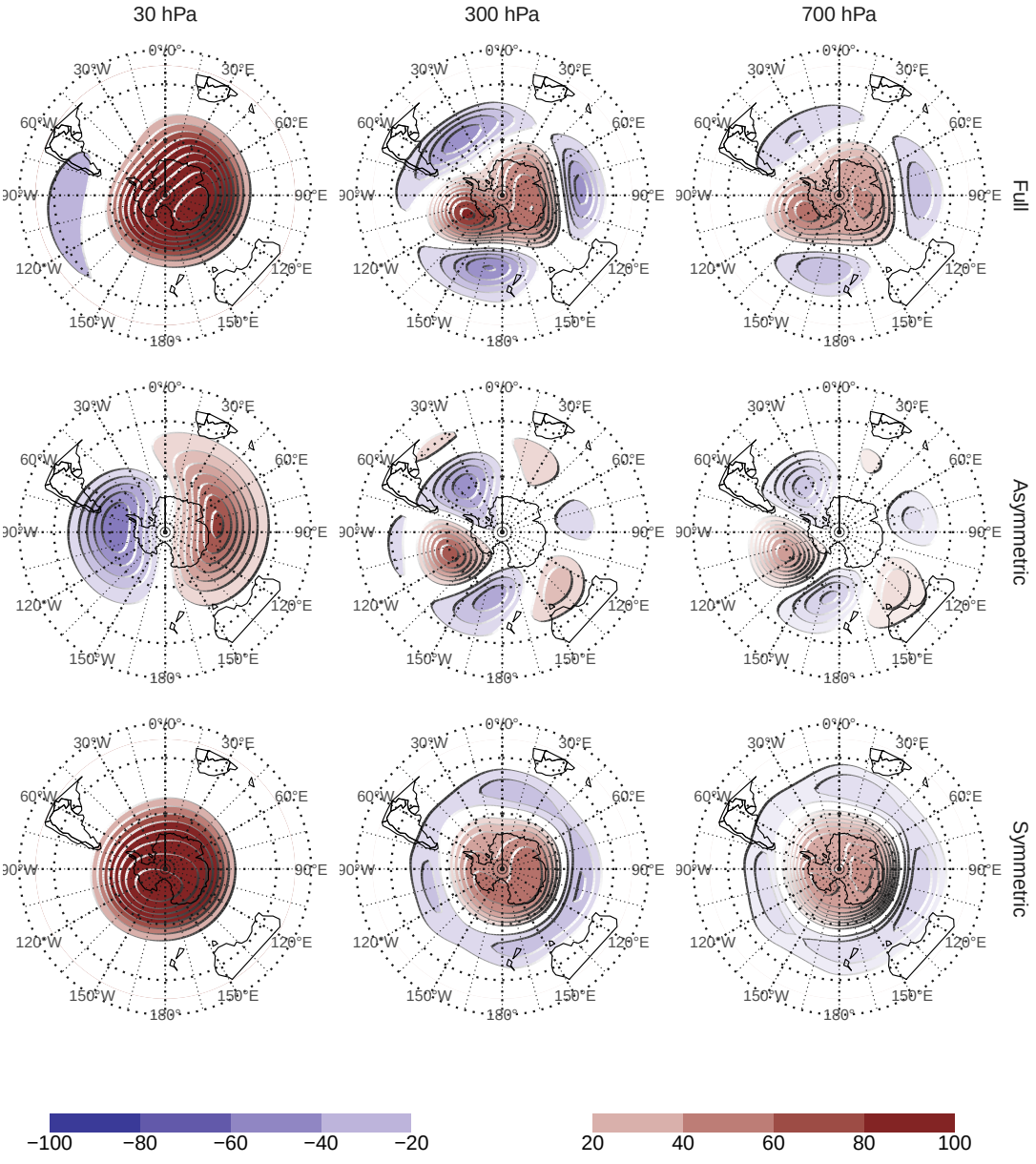

FIG. 9. Regression patterns of geopotential height at 30, 300 and 700 hPa with the Full, Asymmetric and Symmetric SAM. The regression patterns for Asymmetric and Symmetric SAM are the result of one multiple regression using both indices, not of two simple regressions involving each index by itsef.

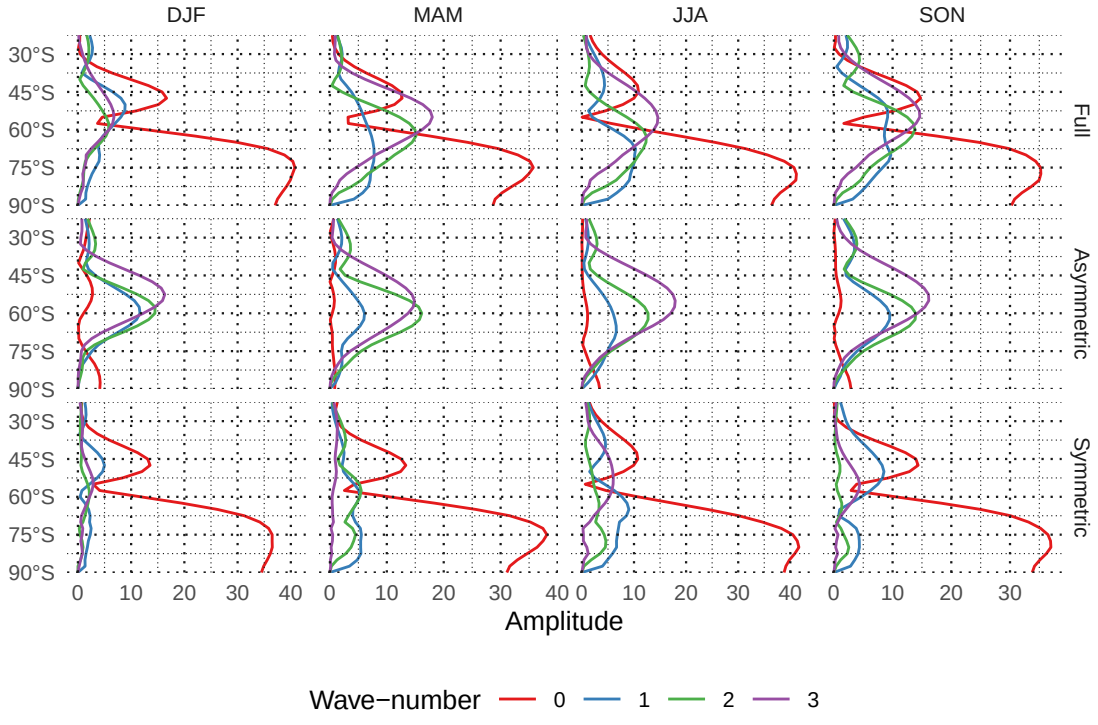

FIG. 10. Planteray wave amplitude for the regression patterns at 700 hPa.

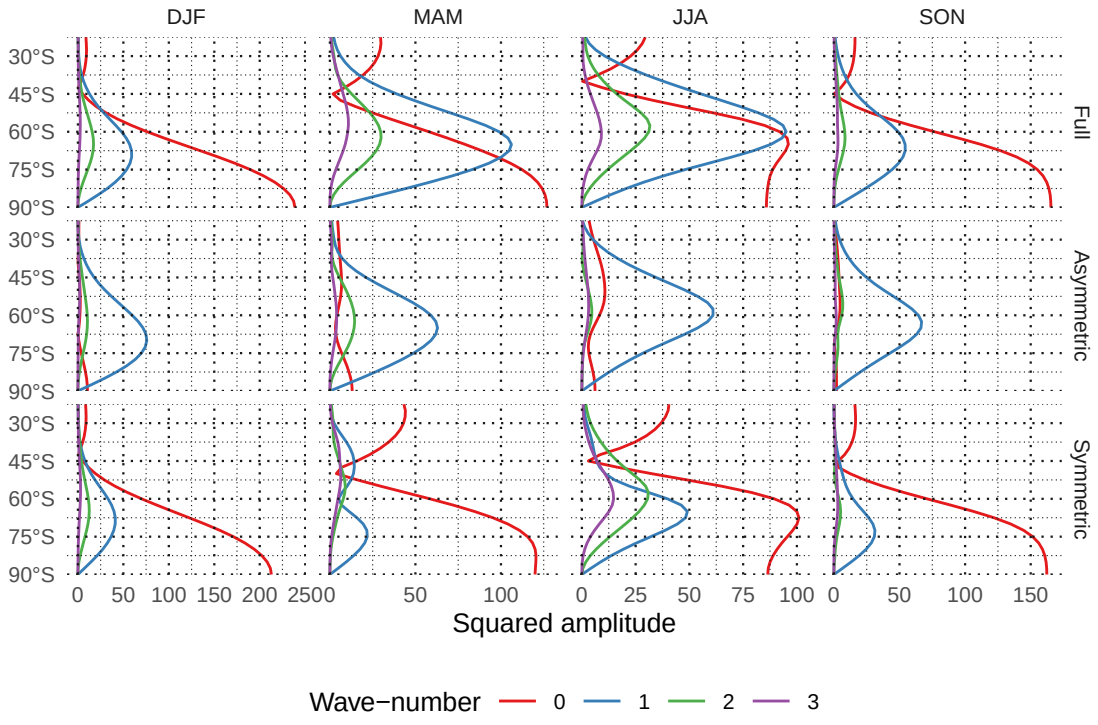

FIG. 11. Planteray wave amplitude for the regression patterns at 30 hPa.

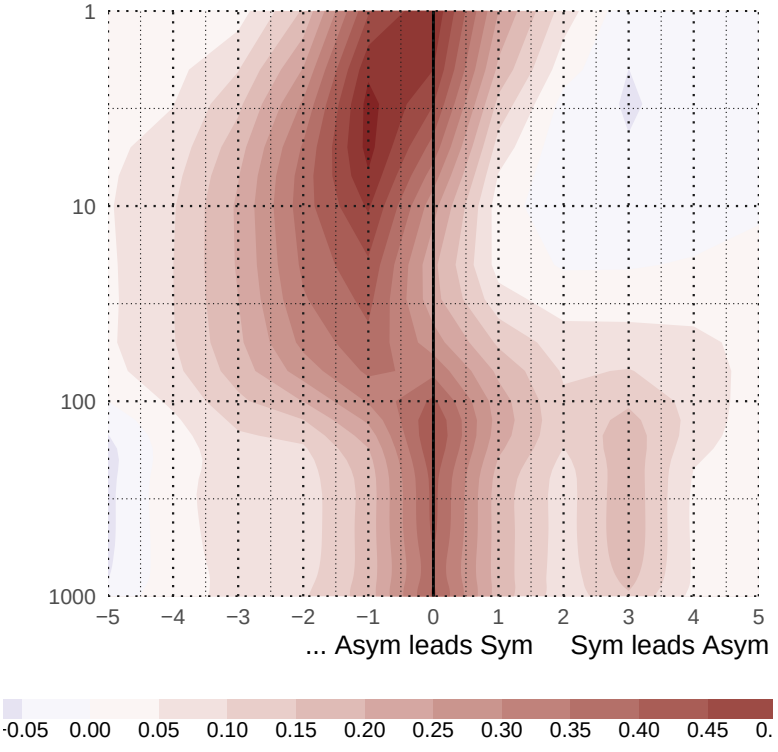

Fig. A1. Lag-correlation between Symmetric and Asymmetric SAM at each level.

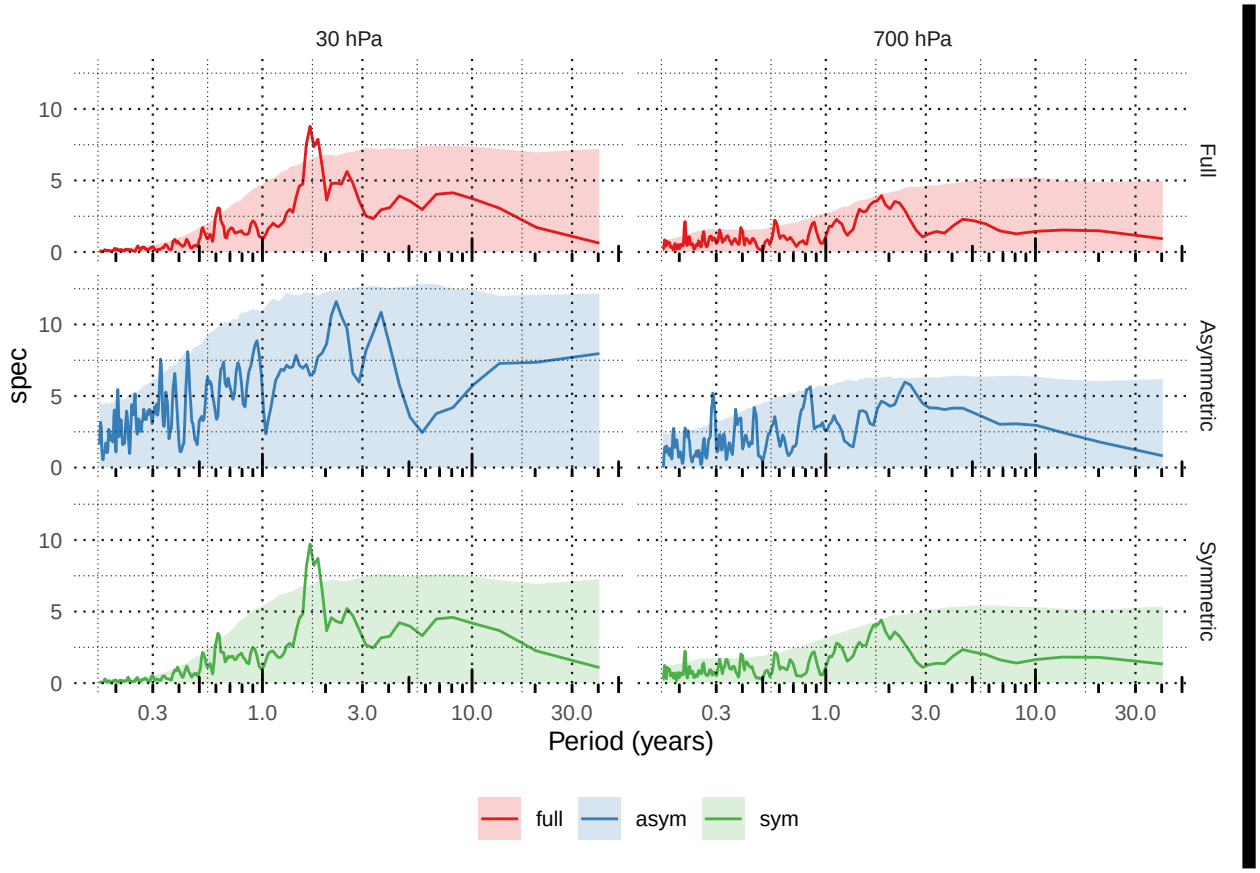

Fig. A2. Fourier spectrum of each timeseries. The shading indicates de 95% qunatile derived fitting an AR process and bootstrapping 5000 simulated samples.

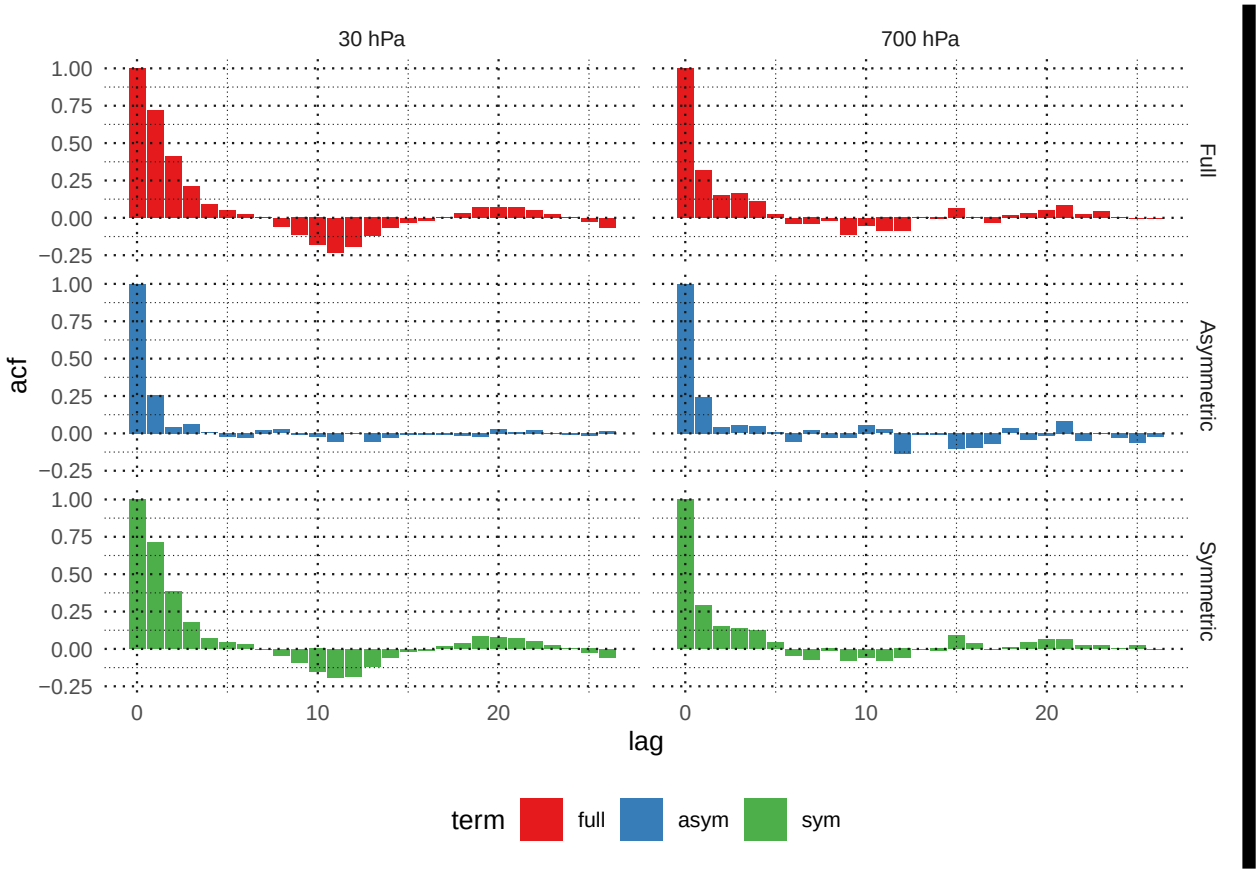

Fig. A3. Autocorrelation functions of each timeseries

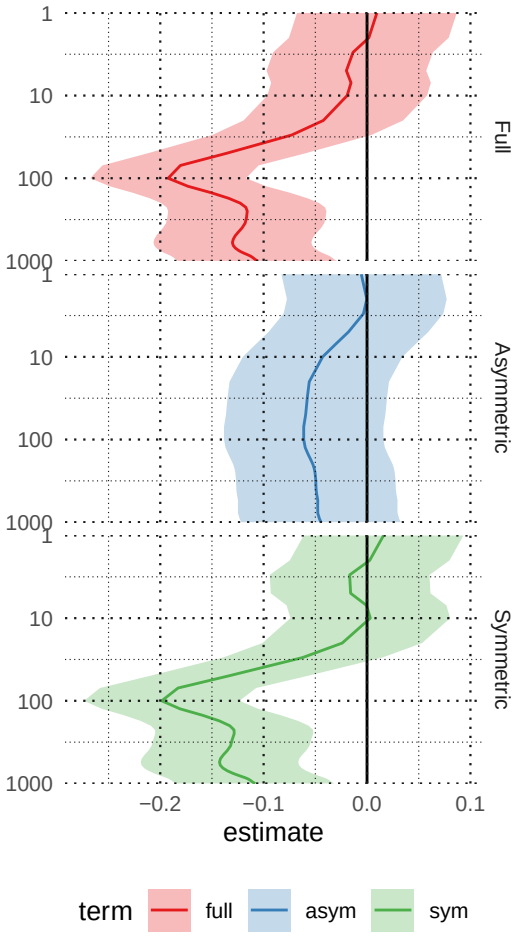

Fig. A4. Trends for each index at each level. Shading indicates the 95% confidence interval.